AGU PUBLICATIONS

Geophysical Research Letters

RESEARCH LETTER
10.1002/2015GL066494

Key Points:
- Skeletal $\delta^{11}B$ and $\delta^{13}C$ are related across four deep-sea coral genera
- $\delta^{13}C$ is strongly related to the difference between coral and seawater pH
- We propose a dual-proxy approach to estimate seawater pH from $\delta^{11}B$ and $\delta^{13}C$

Supporting Information:
- Figure S1
- Table S1
- Table S2

Correspondence to:
P. Martin,
pmartin@ntu.edu.sg

Citation:
Martin, P., N. F. Goodkin, J. A. Stewart, G. L. Foster, E. L. Sikes, H. K. White, S. Hennige, and J. M. Roberts (2016), Deep-sea coral $\delta^{13}C$: A tool to reconstruct the difference between seawater pH and $\delta^{11}B$-derived calcifying fluid pH, *Geophys. Res. Lett.*, *43*, 299–308, doi:10.1002/2015GL066494.

Received 7 OCT 2015
Accepted 12 NOV 2015
Accepted article online 24 NOV 2015
Published online 11 JAN 2016

Deep-sea coral $\delta^{13}C$: A tool to reconstruct the difference between seawater pH and $\delta^{11}B$-derived calcifying fluid pH

Patrick Martin[1,2], Nathalie F. Goodkin[1,2], Joseph A. Stewart[3,4], Gavin L. Foster[3], Elisabeth L. Sikes[5], Helen K. White[6], Sebastian Hennige[7], and J. Murray Roberts[7]

[1]Earth Observatory of Singapore, Singapore, Singapore, [2]Asian School of the Environment, Nanyang Technological University, Singapore, Singapore, [3]Ocean and Earth Science, National Oceanography Centre, University of Southampton, Southampton, UK, [4]Now at National Institute of Standards and Technology, Charleston, South Carolina, USA, [5]Institute of Marine and Coastal Sciences, Rutgers University, New Brunswick, New Jersey, USA, [6]Department of Chemistry, Haverford College, Haverford, Pennsylvania, USA, [7]School of Life Sciences, Heriot-Watt University, Edinburgh, UK

Abstract The boron isotopic composition ($\delta^{11}B$) of coral skeleton is a proxy for seawater pH. However, $\delta^{11}B$-based pH estimates must account for the pH difference between seawater and the coral calcifying fluid, ΔpH. We report that skeletal $\delta^{11}B$ and ΔpH are related to the skeletal carbon isotopic composition ($\delta^{13}C$) in four genera of deep-sea corals collected across a natural pH range of 7.89–8.09, with ΔpH related to $\delta^{13}C$ by $\Delta pH = 0.029 \times \delta^{13}C + 0.929$, $r^2 = 0.717$. Seawater pH can be reconstructed by determining ΔpH from $\delta^{13}C$ and subtracting it from the $\delta^{11}B$-derived calcifying fluid pH. The uncertainty for reconstructions is ±0.12 pH units (2 standard deviations) if estimated from regression prediction intervals or between ±0.04 and ±0.06 pH units if estimated from confidence intervals. Our new approach quantifies and corrects for vital effects, offering improved accuracy relative to an existing $\delta^{11}B$ versus seawater pH calibration with deep-sea scleractinian corals.

1. Introduction

Past changes in atmospheric carbon dioxide concentrations are closely linked to changes in the vast pool of dissolved inorganic carbon in the deep ocean [*Broecker*, 1982; *Burke and Robinson*, 2012; *Martínez-Botí et al.*, 2015; *Sigman and Boyle*, 2000; *Yu et al.*, 2010]. Moreover, human CO_2 emissions are adversely affecting marine ecosystems by reducing seawater pH [*Doney et al.*, 2009; *Gattuso et al.*, 2015]. Directly measured time series of seawater pH only extend back to the 1980s (see *Takahashi et al.* [2014]). Therefore, we are forced to rely on paleoproxies of the seawater carbonate system to better understand natural pH variability in the modern ocean and past ocean-atmosphere CO_2 partitioning [*Goodkin et al.*, 2015; *Hönisch and Hemming*, 2005; *Pelejero et al.*, 2010]. The boron isotope ratio, $\delta^{11}B$, of marine biocarbonates is an important seawater pH proxy [*Hemming*, 2009; *Pelejero and Calvo*, 2007], which has been explored in a range of marine calcifiers, including shallow-water [*Hemming and Hanson*, 1992; *Hönisch et al.*, 2004; *Liu et al.*, 2009] and deep-sea corals [*Anagnostou et al.*, 2012; *Farmer et al.*, 2015; *McCulloch et al.*, 2012b]. However, studies of $\delta^{11}B$ in deep-sea corals have so far been limited to proxy calibration studies [*Anagnostou et al.*, 2012; *Farmer et al.*, 2015] or explorations of coral calcification physiology [*McCulloch et al.*, 2012b]. Paleoceanographic applications of $\delta^{11}B$ to reconstruct ocean-atmosphere CO_2 partitioning have instead mostly relied on foraminifera in sediment cores [*Foster and Sexton*, 2014; *Martínez-Botí et al.*, 2015]. While sediment cores allow paleoceanographic reconstructions that cover extended time periods, their temporal resolution is coarse because sediment accumulation rates in the deep sea are typically only 1–3 cm kyr^{-1}. Expanding paleoceanographic studies of $\delta^{11}B$ to deep-sea coral samples will enable reconstructions of past CO_2 fluxes into and out of the deep ocean carbon pool with much higher temporal resolution.

The application of the $\delta^{11}B$ proxy to corals is complicated by the fact that scleractinian corals elevate the pH of the calcifying fluid (hereafter pH_{cf}) at the site of calcification above the pH of ambient seawater (hereafter pH_{sw}) [*Al-Horani et al.*, 2003; *Venn et al.*, 2011]. This pH upregulation is defined as $\Delta pH = pH_{cf} - pH_{sw}$. Consequently, skeletal $\delta^{11}B$ appears to record pH_{cf}, rather than pH_{sw} [*Holcomb et al.*, 2014; *McCulloch et al.*, 2012a]. pH_{cf} can be calculated directly from skeletal $\delta^{11}B$ using a thermodynamic equation [*Hemming*, 2009], whereas pH_{sw}

can only be estimated from empirical calibrations between skeletal $\delta^{11}B$ and seawater pH. These estimates are possible because pH_{cf} and pH_{sw} are broadly related. However, $\delta^{11}B$ versus pH_{sw} relationships are species specific, implying that the degree of internal pH regulation differs between coral species [*Anagnostou et al*., 2012; *Farmer et al*., 2015; *McCulloch et al*., 2012a; *Trotter et al*., 2011]. Moreover, calcification is an energetically expensive process for corals that is impacted by food supply [*Cohen and Holcomb*, 2009], so it is possible that environmental factors that affect coral physiology also influence the degree of internal pH regulation. Yet empirical calibrations between $\delta^{11}B$ and seawater pH hinge on the assumption that the calcifying fluid pH is a constant function of seawater pH. Any violation of this assumption would introduce errors of unknown magnitude into seawater pH reconstructions.

Several paleo-pH studies with tropical, shallow-water corals of the genus *Porites* have used a different approach, in which the value for the fractionation factor (α) between $B(OH)_3$ and $B(OH)_4^-$ in the thermodynamic equation is reduced to 20‰ [*Douville et al*., 2010; *Hönisch et al*., 2007; *Wei et al*., 2009], instead of using the experimentally derived value of 27.2‰ [*Klochko et al*., 2006]. Reducing α to 20‰ was empirically shown to provide a best fit estimate of pH_{sw} from skeletal $\delta^{11}B$ of the tropical, shallow-water corals *Acropora nobilis* and *Porites compressa* and thus approximately corrects for pH upregulation in these corals [*Hönisch et al*., 2007; *Hönisch et al*., 2004]. A similar empirical approach was taken independently by *Xiao et al*. [2006] using *Acropora* spp., *Pocillopora* spp., a *Montipora* sp., and a *Porites* sp., yielding $\alpha = 20.4‰$. However, an analogous approach has not been developed for deep-sea corals: because of their greater degree of pH upregulation relative to seawater as compared to tropical corals [*McCulloch et al*., 2012b], using $\alpha = 20‰$ would not yield realistic pH_{sw} estimates. To reconstruct pH_{sw} without making assumptions about the magnitude of pH upregulation, a new proxy is needed that records the difference between pH_{cf} and pH_{sw}.

Here we show that the skeletal carbon isotopic composition, $\delta^{13}C$, is closely related to the magnitude of pH upregulation using samples of four deep-sea scleractinian coral genera collected in different parts of the Atlantic and Pacific Oceans that span a natural gradient in pH_{sw}. We further show that this relationship can be used to reconstruct seawater pH using a dual-proxy approach.

2. Methods

2.1. Coral Samples

Twenty-one deep-sea coral specimens were collected from subthermocline depths of 100–1050 m in the Southwest Pacific around New Zealand, the North Atlantic to the west of the United Kingdom, and in the Gulf of Mexico, using dredge hauls (New Zealand corals) or by grab sampling and manned submersibles (Gulf of Mexico and United Kingdom corals). Specimens were from four different genera: *Lophelia pertusa*, *Enallopsammia rostrata*, *Madrepora oculata*, and *Goniocorella dumosa*. Sampling locations are shown in Figure S1 in the supporting information; sampling depths and seawater physicochemical parameters are listed in Table S1. Corals selected for the present analysis were alive when collected. The New Zealand corals were previously analyzed for radiocarbon by *Sikes et al*. [2008]. The collection sites in the Gulf of Mexico were described by *Lunden et al*. [2013] and *White et al*. [2012], and the UK sites by *Findlay et al*. [2014]. For the Gulf of Mexico corals, one coral colony was sampled from each of three sites, and two replicate calyces were analyzed from each colony. All data used in this paper are provided as two supporting information tables.

2.2. Analytical Techniques

An entire coral calyx was selected for analysis from each of the New Zealand and UK corals and removed from the rest of the coral specimen using a Dremel rotary saw. Only a single calyx or half of a calyx (length-wise section) was provided from the Gulf of Mexico specimens. All coral calyces were thoroughly cleaned of residual coral tissue with deionized water using a WaterPik tool or a fine brush and then oven dried overnight (50°C) and crushed to a coarse powder in an agate mortar and pestle. Homogenizing such large amounts of coral material for each sample ensured that samples were representative of average skeletal composition, and biases resulting from microstructural heterogeneities within the sample [see *Allison et al*., 2010 and *Blamart et al*., 2007] were minimized.

Samples were further processed on Class 10 laminar flow benches in a Class 1000 clean laboratory at the University of Southampton following *Foster* [2008] and *Foster et al*. [2013]. For boron analysis, 5–7 mg of coral powder was oxidatively cleaned at 80°C in 1% H_2O_2 buffered to pH 5 with 0.1 M NH_4OH and then subjected to

a weak acid leach in 0.5 mM HNO_3. Cleaned samples were then dissolved in the minimum volume of 0.5 M HNO_3. About 10% of the solution was removed for Mg/Ca and Sr/Ca analysis on a Thermo Scientific Element 2XR inductively coupled plasma mass spectrometer (ICP-MS) against well-characterized, matrix-matched multielement standard solutions (2 σ external precision for Mg/Ca and Sr/Ca was ±1.5%). Boron in the remaining solution was purified using 20 μL microcolumns containing Amberlite IRA 743 anion exchange resin. The boron isotope ratio was measured on a Thermo Scientific Neptune multicollector ICP-MS at the University of Southampton against National Institute of Standards and Technology SRM 951; the long-term precision of the analysis was determined as in *Henehan et al.* [2013] and, in all cases, was better than ±0.21‰ (2 standard deviations, SD).

Calcifying fluid pH was calculated from skeletal $\delta^{11}B$ as

$$pH_{cf} = pK_B - \log\left(\frac{\delta^{11}B_{sw} - \delta^{11}B_{coral}}{\delta^{11}B_{sw} - \alpha\times\delta^{11}B_{coral} - (\alpha - 1)\times 10^3}\right), \quad (1)$$

where $\delta^{11}B_{sw}$ and $\delta^{11}B_{coral}$ are, respectively, the boron isotopic composition of seawater (39.61‰) [*Foster et al.*, 2010] and the coral skeleton, pK_B is the dissociation constant of boric acid (calculated for the appropriate temperature and pressure using the Seacarb R package), and α, the fractionation factor between $B(OH)_3$ and $B(OH)_4^-$, is 1.0272 [*Klochko et al.*, 2006].

The remaining coral powder not used for boron analysis was further ground into a fine powder with an agate mortar and pestle, and 50–80 μg was taken to measure $\delta^{13}C$ and $\delta^{18}O$. Samples were analyzed at the Earth Observatory of Singapore on a Thermo MAT-253 mass spectrometer with a Kiel carbonate device relative to NBS 19; values were expressed on the Vienna Peedee belemnite scale. Analytical precision (1 SD) was evaluated using homogenized marble and was ±0.04‰ for $\delta^{13}C$ and ±0.06‰ for $\delta^{18}O$.

Only a small fraction of each coral sample was used for $\delta^{13}C$ and $\delta^{18}O$ relative to the amount of coral powder available. Therefore, 17 of the 21 samples were analyzed in duplicate for $\delta^{13}C$ and $\delta^{18}O$ to test for sample heterogeneity. Only four samples differed by more than 0.40‰ for $\delta^{13}C$ (0.45–0.64‰) and by more than 0.20‰ for $\delta^{18}O$ (0.21–0.28‰). The remaining duplicate measurements differed by 0.16‰ ($\delta^{13}C$) and 0.06‰ ($\delta^{18}O$) on average. For samples analyzed in duplicate, the final $\delta^{13}C$ and $\delta^{18}O$ values were taken as the mean of both analyses. Error bars in figures for $\delta^{13}C$ and $\delta^{18}O$ show the range of these duplicate measurements.

2.3. Seawater Physicochemical Parameters

The coral samples were collected as part of several different scientific programs, and pH_{sw} was not measured at every site. Where direct measurements were not available, pH_{sw} was calculated from dissolved inorganic carbon (DIC) and total alkalinity (Alk_T) concentrations as described below for each region. All pH values are expressed on the total pH scale. Where pH_{sw} was calculated from DIC and Alk_T, calculations were performed with the Seacarb R package.

2.3.1. Gulf of Mexico

Seawater was collected with Niskin bottles attached to a remotely operated vehicle at the depth of coral collection, and pH_{sw} measured in duplicate on deck at 22°C using an Orion 5 Star pH meter calibrated with Tris buffer, and corrected for temperature and pressure. The reported precision was ±0.002 pH units (1 SD) [*Lunden et al.*, 2013]. The pH values corresponding most closely to the collection depths of the coral colonies used in the present study were provided by J. Lunden (unpublished data, 2010) and fall within the range published by *Lunden et al.* [2013] for each of the sites. Temperature and salinity were taken from the NOAA Gulf of Mexico regional climatology (http://www.nodc.noaa.gov/OC5/regional_climate/GOMclimatology/) and used to calculate pK_B.

2.3.2. Northwest UK

Seawater pH was calculated from measurements of DIC and Alk_T taken in the immediate vicinity of the coral collection sites, using seawater collected with conductivity-temperature-depth rosette-mounted Niskin bottles [*Findlay et al.*, 2014]. These pH estimates agreed closely with estimates based on DIC and Alk_T measurements taken on a hydrographic transect crossing the study area (cruise D379): pH estimates differed by ≤0.02 pH units from the hydrographic transect data at four sites and by 0.10 and 0.12 pH units at the remaining two sites.

2.3.3. New Zealand

Seawater pH and pK_B were calculated from DIC, Alk_T, pressure, salinity, phosphate, and silicic acid data taken from the closest World Ocean Circulation Experiment (WOCE) or Climate and Ocean: Variability, Predictability and Change (CLIVAR) station, or from Global Ocean Data Analysis Project (GLODAP) or WOCE gridded data (see Tables S1 and S2).

2.3.4. Uncertainties in pH and ΔpH Estimates

Analytical uncertainties in T_{Alk} and DIC, and in the direct measurements from the Gulf of Mexico, translate into a final pH_{sw} error of $<$0.01 pH unit. The main source of uncertainty is therefore the degree of temporal variability in seawater chemistry at each site. Because physicochemical parameters in the deep sea are relatively stable over time, these uncertainties should be small. Without repeated measurements of these parameters over time, however, it is difficult to quantify the exact uncertainty of our estimated pH values. The estimates for the New Zealand corals are likely the most error prone, because we had to rely on regional hydrographic data rather than measurements at the coral sites. However, this allows us to draw on multiple measurements from several hydrographic stations for each coral (supporting information Table 2). The standard deviations of these multiple pH estimates at each coral collection site were $<$0.02 pH units, so we use ±0.02 pH units as a conservative estimate of the uncertainty of our pH_{sw} data at all sites—even though we expect that the actual uncertainty of pH_{sw} at our UK and Gulf of Mexico sites would be lower.

The uncertainty of our estimated pH_{cf} values is easier to quantify: the 95% (2 SD) analytical error for $\delta^{11}B$ was $<$0.21‰, so we assume a 1 SD (68% level) uncertainty of ±0.105‰. This translates to a 1 SD uncertainty $\leq$±0.014 pH units in pH_{cf} for all of our coral specimens. pK_B depends on temperature and salinity. It is not straightforward to derive a formal uncertainty estimate for our salinity and temperature data, but variation in both parameters by 0.5 practical salinity units and 0.5°C changes pK_B by $<$0.01. Although we expect that the actual uncertainties in salinity and temperature would be smaller than this, to be conservative, we nevertheless assume a 1 SD error of ±0.01 pH units due to uncertainty in pK_B. Propagating the uncertainty of ±0.01 units from pK_B with the uncertainty of ±0.014 units from $\delta^{11}B$, we obtain a final, propagated 1 SD error of 0.017 pH units for pH_{cf}. Propagating this uncertainty of ±0.017 units for pH_{cf} with the uncertainty in pH_{sw} of ±0.02 units yields an approximate 1 SD uncertainty for ΔpH of ±0.026 pH units.

3. Results and Discussion

3.1. Relationships Between Skeletal $\delta^{11}B$, $\delta^{13}C$, and ΔpH

Skeletal $\delta^{11}B$ and $\delta^{13}C$ showed a significant positive relationship across the entire data set ($r^2 = 0.400$, $p < 0.01$; Figure 1a), which spanned a range of almost 10‰ in $\delta^{13}C$ and 3.5‰ in $\delta^{11}B$. Samples of *Lophelia pertusa* span the entire range of our $\delta^{11}B$ and $\delta^{13}C$ data, indicating that this result is not merely due to species-specific geochemical differences. Moreover, regional differences in $\delta^{13}C$ of DIC between our sampling locations were $<$1‰ according to hydrographic data compiled in the GLODAP data set (UK and New Zealand sites) and measurements by *Aharon et al*. [1992] in the Gulf of Mexico. This is far too small to explain the nearly 10‰ range in our coral data.

Interestingly, correlations between $\delta^{11}B$ and $\delta^{13}C$ have previously been found in the skeletons of shallow-water, symbiotic corals [*Hemming et al*., 1998; *Reynaud et al*., 2004]. *Hemming et al*. [1998] argued that that this correlation arises because seasonal increases in symbiont photosynthesis drive skeletal $\delta^{13}C$ to more positive values and provide more energy for the coral to raise pH_{cf} to higher values. A photosynthesis-based relationship obviously cannot apply to the nonsymbiotic corals examined here, suggesting either that the relationship arises for different reasons in the deep-sea corals or that a common mechanism not linked to photosynthesis is responsible for the relationship in our study as well as the corals examined by *Hemming et al*. [1998] and *Reynaud et al*. [2004].

Unlike previous boron isotope studies in deep-sea corals [*Anagnostou et al*., 2012; *Farmer et al*., 2015], we did not find a direct relationship between skeletal $\delta^{11}B$ and the $\delta^{11}B$ of seawater $B(OH)_4^-$ (Figure 1b). We attribute this to the fact that our data only span 0.2 pH units, while the corals analyzed by *Anagnostou et al*. [2012] and *Farmer et al*. [2015] spanned 0.5 pH units, and the relationships described by these two studies hinge on the samples from low-pH_{sw} conditions. Those samples of *Anagnostou et al*. [2012] that grew in waters with $\delta^{11}B$ of seawater borate $>$15.0‰ show scatter in skeletal $\delta^{11}B$ of about 2‰ (Figure 1b), which is comparable to our data. Moreover, there is no significant correlation between skeletal $\delta^{11}B$ and $\delta^{11}B$ of

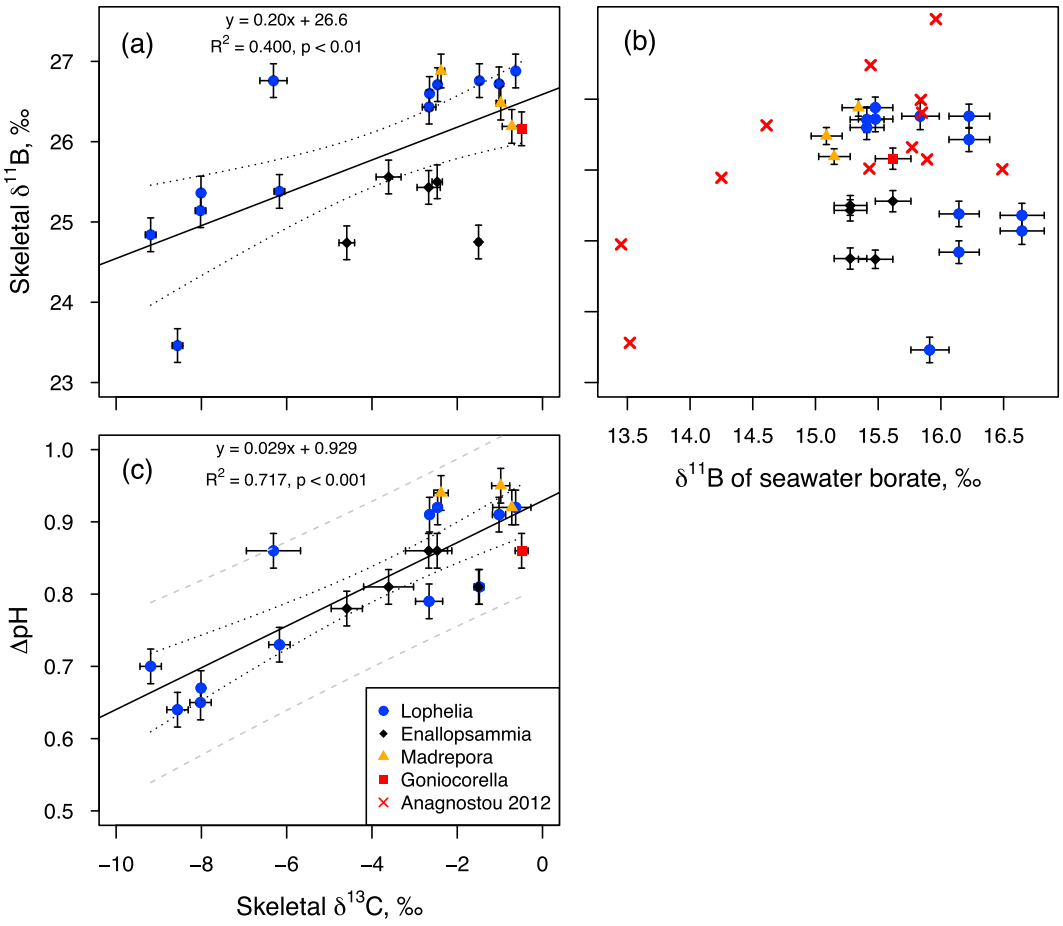

Figure 1. (a) Skeletal δ^{11}B versus δ^{13}C for *Lophelia* (blue circles), *Enallopsammia* (black diamonds), *Madrepora* (orange triangles), and *Goniocorella* (red square). A positive linear regression across all four coral genera is found (solid line; dashed lines indicate 95% confidence intervals). (b) Skeletal δ^{11}B showed no clear relationship to δ^{11}B of seawater $B(OH)_4^-$ across our coral samples. Note that this relationship in the data of *Anagnostou et al.* [2012] hinges on the two samples from waters with lowest δ^{11}B of borate, while over the range of δ^{11}B of borate values in our corals, the *Anagnostou et al.* [2012 (red crosses in panel Figure 1b)] data show similarly high scatter in skeletal δ^{11}B to our corals (error bars were omitted for *Anagnostou et al.* [2012] data for the sake of clarity). (c) Difference in pH between the coral calcification site and seawater (ΔpH) versus skeletal δ^{13}C. A positive linear regression is found (solid line; black dotted lines indicate the 95% confidence interval, and grey dashed lines indicate the 95% prediction interval). Standard errors for, respectively, Figures 1a and 1c are ±0.057 (slope) and ±0.264 (intercept), and ±0.004 (slope) and ±0.019 (intercept). Error bars indicate the 2 SD external reproducibility for δ^{11}B, the range of duplicate analyses for δ^{13}C, and the estimated uncertainties for δ^{11}B of seawater borate (i.e., of pH_{sw}) and of ΔpH as explained in section 2.3.4.

seawater borate if one omits the two data points with lowest δ^{11}B in the *Anagnostou et al.* [2012] data. Omitting these two samples restricts their δ^{11}B of seawater borate to a range slightly greater than in our data set. Similarly, although the data in *Farmer et al.* [2015] show somewhat less scatter, the significance of their skeletal δ^{11}B versus δ^{11}B of seawater borate correlation also hinges on the three low-pH_{sw} samples, if one also omits the outlier value omitted in their analysis (data not shown here owing to the very different δ^{11}B values in the calcitic bamboo corals (gorgonian corals) analyzed by *Farmer et al.* [2015]). Thus, the lack of a relationship in our Figure 1b is perhaps not surprising.

However, there was a strong, positive relationship between ΔpH and skeletal δ^{13}C ($r^2 = 0.717$, $p < 0.001$; Figure 1c). This relationship is most likely the result of vital effects during the calcification process, as we discuss further below. In contrast to our data, skeletal δ^{11}B and δ^{13}C were not related in bamboo corals analyzed by *Farmer et al.* [2015]. However, the bamboo corals showed less pronounced vital effects, with far lower δ^{11}B and ΔpH values than typically found in aragonitic scleractinian corals, suggesting significant differences in calcification physiology between gorgonian and scleractinian corals. Intriguingly, positive relationships between δ^{11}B, δ^{18}O, and δ^{13}C have been reported from *Lophelia pertusa* at the scale of micrometers using an ion microprobe [*Blamart et al.*, 2007; *Rollion-Bard et al.*, 2010], perhaps suggesting that microscale and macroscale measurements of these isotopes reflect the same underlying vital effects.

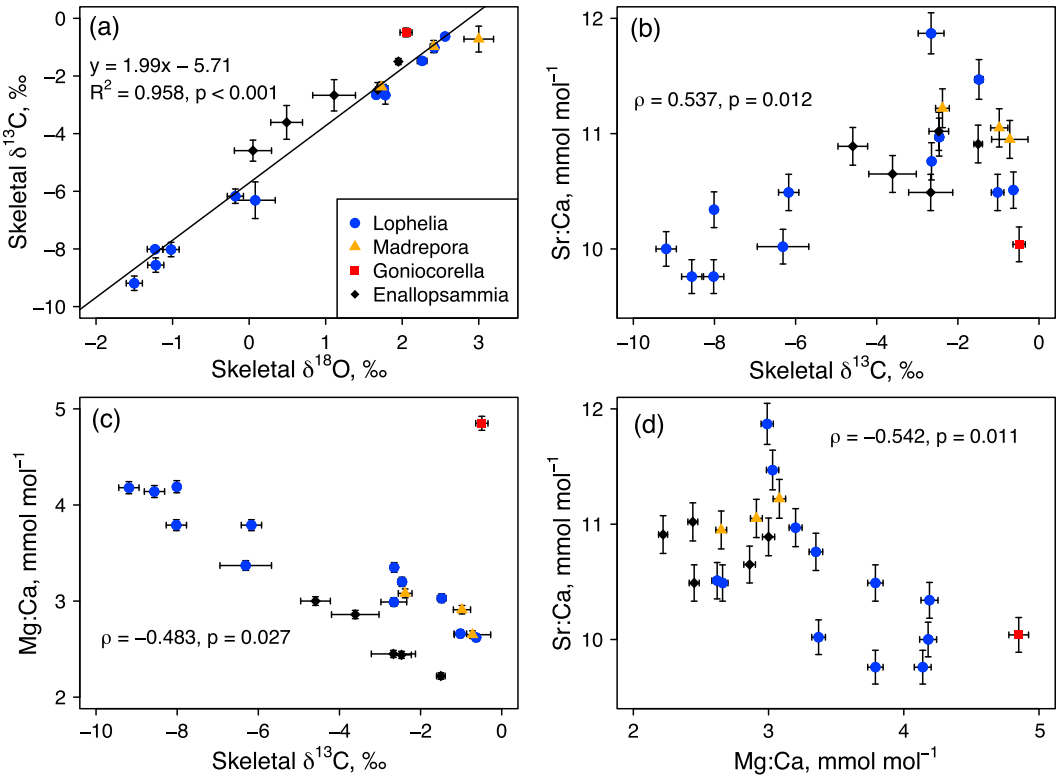

Figure 2. (a) Skeletal $\delta^{13}C$ versus $\delta^{18}O$ is positively related (black line shows linear regression). (b) The skeletal Sr/Ca ratio is positively correlated with skeletal $\delta^{13}C$. (c) The skeletal Mg/Ca ratio is negatively correlated with skeletal $\delta^{13}C$. (d) Skeletal Sr/Ca and Mg/Ca are negatively correlated. Spearman's rank correlations are shown in Figures 2b–2d. Error bars indicate the range of duplicate measurements for $\delta^{13}C$ and $\delta^{18}O$, and the 2 SD external reproducibility of ±1.5% for Sr/Ca and Mg/Ca.

3.2. Estimating Seawater pH From $\delta^{11}B$ and $\delta^{13}C$

Our data point toward a new, dual-proxy method of estimating pH_{sw}: first, pH_{cf} is calculated from skeletal $\delta^{11}B$ as described in section 2.2. Second, ΔpH is calculated from skeletal $\delta^{13}C$ according to the relationship in Figure 1c and subtracted from the corresponding pH_{cf} value. We formally estimate the accuracy of this approach by propagating the 68% (1 SD) prediction interval of the ΔpH versus $\delta^{13}C$ regression model and our estimated 1 SD uncertainty for $\delta^{11}B$-based pH_{cf} estimates. The latter was ±0.017 pH units, while the former ranges from ±0.056 (at $\delta^{13}C = -3.6‰$) to ±0.060 (at $\delta^{13}C = -9.0‰$). Combining these two errors using the sum of squares gives a final estimate of uncertainty for individual pH estimates based on $\delta^{11}B$ and $\delta^{13}C$ between ±0.059 and ±0.062 pH units at the 1 SD level, or ±0.117 to ±0.125 at the 2 SD level, depending on the value of $\delta^{13}C$.

The prediction interval of a regression is distinct from the confidence interval: the former is an estimate of the uncertainty with which new, individual predictions can be made from a regression, while the latter indicates the uncertainty with which the population mean can be predicted at a given *x* value (i.e., the uncertainty of the regression line). Both types of interval are indicated in Figure 1c. The prediction interval is necessarily larger than the confidence interval: had we used the confidence interval of our ΔpH versus $\delta^{13}C$ relationship instead of the prediction interval to estimate the final uncertainty of pH_{sw} (as was done by *Anagnostou et al.* [2012]), our final 1 SD uncertainty would have been between ±0.0208 and ±0.0308 pH units, corresponding to a 2 SD uncertainty of between ±0.042 and ±0.062 pH units. Our dual-proxy approach thus offers improved accuracy relative to the existing deep-sea coral calibration and does not assume that coral vital effects are a constant function of seawater pH. Additional data are needed to better constrain the ΔpH versus $\delta^{13}C$ relationship and improve the accuracy of our approach further. In particular, it would be valuable to extend our observations with samples covering a greater pH_{sw} range than the 0.2 pH units covered by our data set.

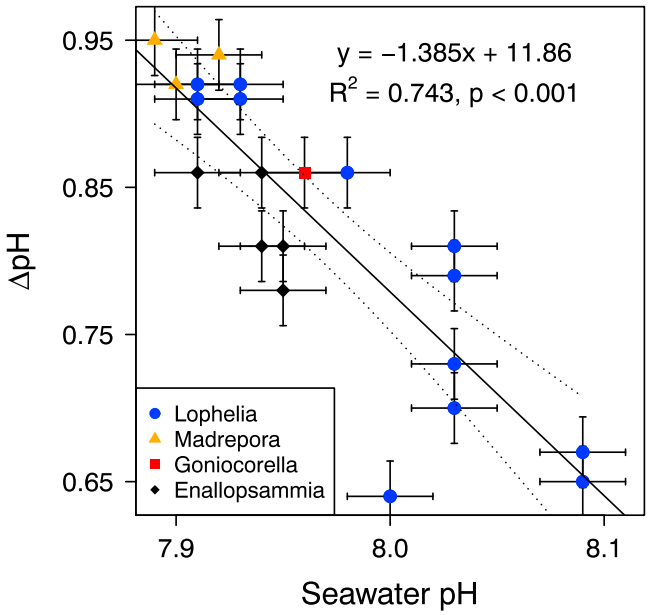

Figure 3. ΔpH and seawater pH show a strong, negative relationship, indicating that the corals compensate for lower seawater pH by raising their calcifying fluid pH. The solid line shows the regression line, and dashed lines are the 95% confidence interval. Error bars indicate the estimated uncertainty for ΔpH and pH_{sw} as described in section 2.3.4.

3.3. Mechanisms Linking $\delta^{13}C$ and ΔpH

To further investigate the cause for the ΔpH–$\delta^{13}C$ relationship, we examined the skeletal oxygen isotope composition ($\delta^{18}O$), and the Sr/Ca and Mg/Ca ratios. We found a strong, positive relationship between $\delta^{18}O$ and $\delta^{13}C$ (Figure 2a), consistent with previous coral data, and indicative of strong vital effects likely related to coral pH upregulation [*Adkins et al.*, 2003; *McConnaughey*, 1989; *Spiro et al.*, 2000]. While hypotheses to explain these vital effects differ in their details [*Adkins et al.*, 2003; *Marali et al.*, 2013; *McConnaughey*, 1989; *Rollion-Bard et al.*, 2010], it is generally thought that corals regulate the calcification rate by modulating their calcification site pH, and that skeletal $\delta^{13}C$ and $\delta^{18}O$ are more negative under conditions of more rapid calcification/elevated calcification site pH. For $\delta^{13}C$, this is most likely because depletion of DIC and elevated pH_{cf} promote the diffusion of CO_2 from seawater to the calcifying fluid, where the CO_2 then reacts to form aragonite. CO_2 has a light carbon isotopic composition relative to the total DIC pool [*Zhang et al.*, 1995], and aragonite formed from diffused CO_2 consequently has a more negative $\delta^{13}C$ value.

If our $\delta^{13}C$ data are indeed driven by these vital effects, then more negative $\delta^{13}C$ values would indicate that the rate at which fresh seawater is brought to the calcifying fluid is slow relative to the rate at which new skeleton is deposited, i.e., that conditions are more closed system like with regard to seawater exchange. We find a positive correlation between Sr/Ca and $\delta^{13}C$, a negative correlation between Mg/Ca and $\delta^{13}C$, and a negative correlation between Sr/Ca and Mg/Ca (Figures 2b–2d). Inverse correlations between Sr/Ca and Mg/Ca have been interpreted as indicating Rayleigh fractionation [*Gaetani et al.*, 2011; *Gagnon et al.*, 2007; *Tanaka et al.*, 2015]. While this interpretation for Mg may be inaccurate, because Mg is not directly incorporated into the aragonite lattice [*Finch and Allison*, 2008], Sr has a partition coefficient into coral aragonite >1, so the greater the proportion of the calcifying fluid that precipitates, the lower the resulting aragonite Sr/Ca will be. Our positive correlation between Sr/Ca and $\delta^{13}C$ thus indicates that samples with lower $\delta^{13}C$ were formed when a large proportion of the calcifying fluid was precipitated relative to the rate at which the calcifying fluid was replenished with seawater. The low $\delta^{13}C$ of these samples most likely indicates greater diffusion of molecular CO_2 to the calcifying fluid.

Our data show that lower $\delta^{13}C$ and $\delta^{18}O$ values were found at lower rather than higher ΔpH values, potentially implying that corals with lower ΔpH values in fact had a faster calcification rate than corals with higher ΔpH. This may seem at odds with the presumed association of high pH_{cf} with high CO_3^{2-} concentrations in

the calcifying fluid and hence rapid $CaCO_3$ precipitation. However, ΔpH was inversely related to pH_{sw} in our corals (Figure 3), consistent with the direct observations by *Venn et al*. [2013] that corals maintain a greater ΔpH when cultured at lower pH_{sw}. Despite the caveat that ΔpH and pH_{sw} are not technically independent of each other, our ΔpH, pH_{sw}, and $\delta^{13}C$ data (Figures 1c and 3) are consistent with the intuitive idea that corals growing under low-pH conditions probably calcify more slowly than corals growing at high-pH sites, in spite of internal pH upregulation. This is again consistent with the observations by *Venn et al*. [2013] that calcification rate is reduced at lower pH_{sw} despite increasing ΔpH, although the reduction was only statistically significant in the lowest pH_{sw} treatment owing to high variability between replicate colonies. Direct estimates of calcification rates in deep-sea corals would be needed to further confirm the mechanism underlying the geochemical relationships in our corals.

3.4. Paleoceanographic Importance

Past changes in atmospheric CO_2 concentrations, such as over glacial-interglacial time scales, are largely attributed to changes in carbon storage in the deep ocean [*Martínez-Botí et al*., 2015; *Yu et al*., 2010]. However, the mechanisms and constraints on the timing, magnitude, and location of deep ocean carbon storage are still debated. The pH in the deep sea probably varied by no more than 0.15 pH units between glacial and interglacial periods [*Hönisch et al*., 2008; *Martínez-Botí et al*., 2015; *Rae et al*., 2014]. The magnitude of these changes is therefore still comparable to our (conservative) estimate of uncertainty for the dual-proxy approach. However, our study is based on only 21 corals spanning a limited pH range of 0.2 units, and we expect that further work to expand our data set may improve the accuracy of the method. Reconstructing past variations in seawater pH by measuring $\delta^{11}B$ in the many archived deep-sea coral samples [*Robinson et al*., 2005] could then provide records of past seawater CO_2 concentration with much higher temporal resolution than can be obtained from foraminifera in sediment cores. This, in turn, would help to shed light on the relative roles of different oceanic CO_2 storage mechanisms during periods of major climatic change.

4. Conclusions

We have found strong, positive relationships between $\delta^{11}B$, ΔpH, and $\delta^{13}C$ in a set of deep-sea corals comprising four different genera collected in three different ocean regions. Importantly, the relationship between skeletal $\delta^{13}C$ and ΔpH appears robust across a wide range of environments and possibly four coral genera, allowing the ambient seawater pH at which the corals grew to be estimated with a 2 SD uncertainty of $\leq \pm 0.125$ pH units. This conservative estimate of uncertainty is based on regression prediction intervals and is twofold to threefold higher than the estimate based on regression confidence intervals, which is ±0.042–0.062 pH units. Thus, the dual-proxy approach already represents an improvement in accuracy over existing deep-sea coral $\delta^{11}B$ versus pH_{sw} calibrations. With further refinement, this may prove to be a promising approach for seawater pH reconstructions.

Acknowledgments

N.F.G. and P.M. were funded by the National Research Foundation Singapore under its Singapore NRF Fellowship scheme awarded to N.F. Goodkin (National Research Fellow award NRF-RF2012-03), as administered by the Earth Observatory of Singapore and the Singapore Ministry of Education under the Research Centres of Excellence initiative. G.L. Foster, J.A. Stewart, M. Roberts, and S.J. Hennige acknowledge the support of NERC via NE/J021075/1, NE/H017305/1, and NE/K009028/1. The New Zealand National Institute for Water and Atmospheric Research donated coral specimens. The captains and crew of R/V *Atlantis*, RRS *Discovery* (D366), RRS *James Cook* (JC073), and the pilots of submersibles DSV *Alvin* and *Pisces* III helped collect the Gulf of Mexico and UK corals. We thank T.T. Yang for initiating this project, J. Lunden and H. Findlay for sharing seawater pH data, E. Anagnostou and A. Bolton for helpful comments, and S.-H. Ng and R. He for help with $\delta^{13}C$ and $\delta^{18}O$ analysis. We thank N. Allison and one anonymous reviewer for constructive criticism. All data used in this paper are provided as two supporting information tables.

References

Adkins, J. F., E. A. Boyle, W. B. Curry, and A. Lutringer (2003), Stable isotopes in deep-sea corals and a new mechanism for "vital effects", *Geochim. Cosmochim. Acta*, *67*(6), 1129–1143, doi:10.1016/S0016-7037(00)01203-6.

Aharon, P., E. R. Graber, and H. H. Roberts (1992), Dissolved carbon and $\delta^{13}C$ anomalies in the water column caused by hydrocarbon seeps on the northwestern Gulf of Mexico slope, *Geo-Mar. Lett.*, *12*(1), 33–40, doi:10.1007/BF02092106.

Al-Horani, F. A., S. M. Al-Moghrabi, and D. de Beer (2003), Microsensor study of photosynthesis and calcification in the scleractinian coral, *Galaxea fascicularis*: Active internal carbon cycle, *J. Exp. Mar. Biol. Ecol.*, *288*, 1–15, doi:10.1016/S0022-0981(02)00578-6.

Allison, N., A. A. Finch, and EIMF (2010), $\delta^{11}B$, Sr, Mg and B in a modern *Porites* coral: The relationship between calcification site pH and skeletal chemistry, *Geochim. Cosmochim. Acta*, *74*(6), 1790–1800, doi:10.1016/J.Gca.2009.12.030.

Anagnostou, E., K. F. Huang, C. F. You, E. L. Sikes, and R. M. Sherrell (2012), Evaluation of boron isotope ratio as a pH proxy in the deep sea coral *Desmophyllum dianthus*: Evidence of physiological pH adjustment, *Earth Planet. Sci. Lett.*, *349–350*, 251–260, doi:10.1016/j.epsl.2012.07.006.

Blamart, D., C. Rollion-Bard, A. Meibom, J. P. Cuif, A. Juillet-Leclerc, and Y. Dauphin (2007), Correlation of boron isotopic composition with ultrastructure in the deep-sea coral *Lophelia pertusa*: Implications for biomineralization and paleo-pH, *Geochem. Geophys. Geosyst.*, *8*, Q12001, doi:10.1029/2007GC001686.

Broecker, W. S. (1982), Glacial to interglacial changes in ocean chemistry, *Prog. Oceanogr.*, *11*(2), 151–197.

Burke, A., and L. F. Robinson (2012), The Southern Ocean's role in carbon exchange during the last deglaciation, *Science*, *335*(6068), 557–561, doi:10.1126/science.1208163.

Cohen, A. L., and M. Holcomb (2009), Why corals care about ocean acidification: Uncovering the mechanism, *Oceanography*, *22*(4), 118–127.

Doney, S. C., V. J. Fabry, R. A. Feely, and J. A. Kleypas (2009), Ocean acidification: The other CO_2 problem, *Annu. Rev. Mar. Sci.*, *1*(1), 169–192, doi:10.1146/annurev.marine.010908.163834.

Douville, E., M. Paterne, G. Cabioch, P. Louvat, J. Gaillardet, A. Juillet-Leclerc, and L. Ayliffe (2010), Abrupt sea surface pH change at the end of the Younger Dryas in the central sub-equatorial Pacific inferred from boron isotope abundance in corals (*Porites*), *Biogeosciences*, *7*(8), 2445–2459, doi:10.5194/Bg-7-2445-2010.

Farmer, J. R., B. Hönisch, L. F. Robinson, and T. M. Hill (2015), Effects of seawater-pH and biomineralization on the boron isotopic composition of deep-sea bamboo corals, *Geochim. Cosmochim. Acta*, *155*, 86–106, doi:10.1016/j.gca.2015.01.018.

Finch, A. A., and N. Allison (2008), Mg structural state in coral aragonite and implications for the paleoenvironmental proxy, *Geophys. Res. Lett.*, *35*, L08704, doi:10.1029/2008GL033543.

Findlay, H. S., S. J. Hennige, L. C. Wicks, J. M. Navas, E. M. S. Woodward, and J. M. Roberts (2014), Fine-scale nutrient and carbonate system dynamics around cold-water coral reefs in the northeast Atlantic, *Sci. Rep.*, *4*, 3671–3681, doi:10.1038/srep03671.

Foster, G. L. (2008), Seawater pH, pCO_2 and $[CO_3^{-2}]$ variations in the Caribbean Sea over the last 130 kyr: A boron isotope and B/Ca study of planktic foraminifera, *Earth Planet. Sci. Lett.*, *271*(1–4), 254–266, doi:10.1016/j.epsl.2008.04.015.

Foster, G. L., and P. F. Sexton (2014), Enhanced carbon dioxide outgassing from the eastern equatorial Atlantic during the last glacial, *Geology*, *42*(11), 1003–1006.

Foster, G. L., P. A. E. Pogge von Strandmann, and J. W. B. Rae (2010), Boron and magnesium isotopic composition of seawater, *Geochem. Geophys. Geosyst.*, *11*, Q08015, doi:10.1029/2010GC003201.

Foster, G. L., B. Hönisch, G. Paris, G. S. Dwyer, J. W. B. Rae, T. Elliott, J. Gaillardet, N. G. Hemming, P. Louvat, and A. Vengosh (2013), Interlaboratory comparison of boron isotope analyses of boric acid, seawater and marine $CaCO_3$ by MC-ICPMS and NTIMS, *Chem. Geol.*, *358*, 1–14, doi:10.1016/j.chemgeo.2013.08.027.

Gaetani, G. A., A. L. Cohen, Z. Wang, and J. Crusius (2011), Rayleigh-based, multi-element coral thermometry: A biomineralization approach to developing climate proxies, *Geochim. Cosmochim. Acta*, *75*(7), 1920–1932, doi:10.1016/j.gca.2011.01.010.

Gagnon, A. C., J. F. Adkins, D. P. Fernandez, and L. F. Robinson (2007), Sr/Ca and Mg/Ca vital effects correlated with skeletal architecture in a scleractinian deep-sea coral and the role of Rayleigh fractionation, *Earth Planet. Sci. Lett.*, *261*(1–2), 280–295, doi:10.1016/j.epsl.2007.07.013.

Gattuso, J. P., et al. (2015), Contrasting futures for ocean and society from different anthropogenic CO_2 emissions scenarios, *Science*, *349*(6243), doi:10.1126/science.aac4722.

Goodkin, N. F., B.-S. Wang, C.-F. You, K. A. Hughen, N. Grumet-Prouty, N. R. Bates, and S. C. Doney (2015), Ocean circulation and biogeochemistry moderate inter-annual and decadal surface water pH changes in the Sargasso Sea, *Geophys. Res. Lett.*, 4931–4939, doi:10.1002/2015GL064431.

Hemming, N. G. (2009), Isotopes illuminate chemical change: Boron isotope pH proxy, in *Chemical Evolution II: From the Origins of Life to Modern Society*, edited by L. Zaikowski, J. M. Friedrich, and R. S. Seidel, pp. 157–177, Am. Chem. Soc, Washington, D. C.

Hemming, N. G., and G. N. Hanson (1992), Boron isotopic composition and concentration in modern marine carbonates, *Geochim. Cosmochim. Acta*, *56*(1), 537–543, doi:10.1016/0016-7037(92)90151-8.

Hemming, N. G., T. P. Guilderson, and R. G. Fairbanks (1998), Seasonal variations in the boron isotopic composition of coral: A productivity signal?, *Global Biogeochem. Cycles*, *12*(4), 581–586.

Henehan, M. J., et al. (2013), Calibration of the boron isotope proxy in the planktonic foraminifera *Globigerinoides ruber* for use in palaeo-CO_2 reconstruction, *Earth Planet. Sci. Lett.*, *364*, 111–122, doi:10.1016/j.epsl.2012.12.029.

Holcomb, M., A. A. Venn, E. Tambutte, S. Tambutte, D. Allemand, J. Trotter, and M. McCulloch (2014), Coral calcifying fluid pH dictates response to ocean acidification, *Sci. Rep.*, *4*, doi:10.1038/srep05207.

Hönisch, B., and N. G. Hemming (2005), Surface ocean pH response to variations in pCO_2 through two full glacial cycles, *Earth Planet. Sci. Lett.*, *236*(1–2), 305–314, doi:10.1016/j.epsl.2005.04.027.

Hönisch, B., N. G. Hemming, A. G. Grottoli, A. Amat, G. N. Hanson, and J. Bijma (2004), Assessing scleractinian corals as recorders for paleo-pH: Empirical calibration and vital effects, *Geochim. Cosmochim. Acta*, *68*(18), 3675–3685, doi:10.1016/j.gca.2004.03.002.

Hönisch, B., N. G. Hemming, and B. Loose (2007), Comment on "A critical evaluation of the boron isotope-pH proxy: The accuracy of ancient ocean pH estimates" by M. Pagani, D. Lemarchand, A. Spivack and J. Gaillardet, *Geochim. Cosmochim. Acta*, *71*, 1636–1641.

Hönisch, B., T. Bickert, and N. G. Hemming (2008), Modern and Pleistocene boron isotope composition of the benthic foraminifer *Cibicidoides wuellerstorfi*, *Earth Planet. Sci. Lett.*, *272*(1–2), 309–318, doi:10.1016/j.epsl.2008.04.047.

Klochko, K., A. J. Kaufman, W. Yao, R. H. Byrne, and J. A. Tossell (2006), Experimental measurement of boron isotope fractionation in seawater, *Earth Planet. Sci. Lett.*, *248*(1–2), 276–285, doi:10.1016/j.epsl.2006.05.034.

Liu, Y., W. Liu, Z. Peng, Y. Xiao, G. Wei, W. Sun, J. He, G. Liu, and C.-L. Chou (2009), Instability of seawater pH in the South China Sea during the mid-late Holocene: Evidence from boron isotopic composition of corals, *Geochim. Cosmochim. Acta*, *73*(5), 1264–1272, doi:10.1016/j.gca.2008.11.034.

Lunden, J. J., S. E. Georgian, and E. E. Cordes (2013), Aragonite saturation states at cold-water coral reefs structured by *Lophelia pertusa* in the northern Gulf of Mexico, *Limnol. Oceanogr.*, *58*(1), 354–362, doi:10.4319/lo.2013.58.1.0354.

Marali, S., M. Wisshak, M. López Correa, and A. Freiwald (2013), Skeletal microstructure and stable isotope signature of three bathyal solitary cold-water corals from the Azores, *Palaeogeogr. Palaeoclimatol. Palaeoecol.*, *373*, 25–38, doi:10.1016/j.palaeo.2012.06.017.

Martínez-Botí, M. A., G. Marino, G. L. Foster, P. Ziveri, M. J. Henehan, J. W. B. Rae, P. G. Mortyn, and D. Vance (2015), Boron isotope evidence for oceanic carbon dioxide leakage during the last deglaciation, *Nature*, *518*(7538), 219–222, doi:10.1038/nature14155.

McConnaughey, T. A. (1989), ^{13}C and ^{18}O Isotopic disequilibrium in biological carbonates: 1. Patterns, *Geochim. Cosmochim. Acta*, *53*(1), 151–162, doi:10.1016/0016-7037(89)90282-2.

McCulloch, M., J. Falter, J. Trotter, and P. Montagna (2012a), Coral resilience to ocean acidification and global warming through pH up-regulation, *Nat. Clim. Change*, *2*, 623–627, doi:10.1038/NCLIMATE1473.

McCulloch, M., et al. (2012b), Resilience of cold-water scleractinian corals to ocean acidification: Boron isotopic systematics of pH and saturation state up-regulation, *Geochim. Cosmochim. Acta*, *87*, 21–34, doi:10.1016/j.gca.2012.03.027.

Pelejero, C., and E. Calvo (2007), Reconstructing past seawater pH from boron isotopes in carbonates, *Contrib. Sci.*, *3*, 385–394.

Pelejero, C., E. Calvo, and O. Hoegh-Guldberg (2010), Paleo-perspectives on ocean acidification, *Trends Ecol. Evol.*, *25*(6), 332–344, doi:10.1016/j.tree.2010.02.002.

Rae, J. W. B., M. Sarnthein, G. L. Foster, A. J. Ridgwell, P. M. Grootes, and T. Elliott (2014), Deep water formation in the North Pacific and deglacial CO_2 rise, *Paleoceanography*, *29*, 645–667, doi:10.1002/2013PA002570.

Reynaud, S., N. G. Hemming, A. Juillet-Leclerc, and J.-P. Gattuso (2004), Effect of pCO_2 and temperature on the boron isotopic composition of the zooxanthellate coral *Acropora* sp, *Coral Reefs*, *23*, 539–546, doi:10.1007/s00338-004-0399-5.

Robinson, L. F., J. F. Adkins, L. D. Keigwin, J. Southon, D. P. Fernandez, S. L. Wang, and D. S. Scheirer (2005), Radiocarbon variability in the western North Atlantic during the last deglaciation, *Science*, *310*(5753), 1469–1473, doi:10.1126/science.1114832.

Rollion-Bard, C., D. Blamart, J.-P. Cuif, and Y. Dauphin (2010), *In situ* measurements of oxygen isotopic composition in deep-sea coral, *Lophelia pertusa*: Re-examination of the current geochemical models of biomineralization, *Geochim. Cosmochim. Acta*, *74*(4), 1338–1349, doi:10.1016/j.gca.2009.11.011.

Sigman, D. M., and E. A. Boyle (2000), Glacial/interglacial variations in atmospheric carbon dioxide, *Nature*, *407*(6806), 859–869.
Sikes, E. L., S. N. Burgess, R. Grandpre, and T. P. Guilderson (2008), Assessing modern deep-water ages in the New Zealand region using deep-water corals, *Deep Sea Res., Part I*, *55*(1), 38–49, doi:10.1016/j.dsr.2007.10.004.
Spiro, B., M. Roberts, J. Gage, and S. Chenery (2000), $^{18}O/^{16}O$ and $^{13}C/^{12}C$ in an ahermatypic deep-water coral *Lophelia pertusa* from the North Atlantic: A case of disequilibrium isotope fractionation, *Rapid Commun. Mass Spectrom.*, *14*(15), 1332–1336.
Takahashi, T., S. C. Sutherland, D. W. Chipman, J. G. Goddard, C. Ho, T. Newberger, C. Sweeney, and D. R. Munro (2014), Climatological distributions of pH, pCO_2, total CO_2, alkalinity, and $CaCO_3$ saturation in the global surface ocean, and temporal changes at selected locations, *Mar. Chem.*, *164*, 95–125, doi:10.1016/j.marchem.2014.06.004.
Tanaka, K., M. Holcomb, A. Takahashi, H. Kurihara, R. Asami, R. Shinjo, K. Sowa, K. Rankenburg, T. Watanabe, and M. McCulloch (2015), Response of *Acropora digitifera* to ocean acidification: Constraints from $\delta^{11}B$, Sr, Mg, and Ba compositions of aragonitic skeletons cultured under variable seawater pH, *Coral Reefs*, *34*(4), 1139–1149, doi:10.1007/s00338-015-1319-6.
Trotter, J., P. Montagna, M. McCulloch, S. Silenzi, S. Reynaud, G. Mortimer, S. Martin, C. Ferrier-Pagès, J.-P. Gattuso, and R. Rodolfo-Metalpa (2011), Quantifying the pH 'vital effect' in the temperate zooxanthellate coral *Cladocora caespitosa*: Validation of the boron seawater pH proxy, *Earth Planet. Sci. Lett.*, *303*(3–4), 163–173, doi:10.1016/j.epsl.2011.01.030.
Venn, A. A., E. Tambutté, M. Holcomb, J. Laurent, D. Allemand, and S. Tambutté (2013), Impact of seawater acidification on pH at the tissue-skeleton interface and calcification in reef corals, *Proc. Natl. Acad. Sci. U.S.A.*, *110*(5), 1634–1639, doi:10.1073/pnas.1216153110.
Venn, A., E. Tambutté, M. Holcomb, D. Allemand, and S. Tambutté (2011), Live tissue imaging shows reef corals elevate pH under their calcifying tissue relative to seawater, *PLoS One*, *6*(5), doi:10.1371/journal.pone.0020013.
Wei, G., M. T. McCulloch, G. Mortimer, W. Deng, and L. Xie (2009), Evidence for ocean acidification in the Great Barrier Reef of Australia, *Geochim. Cosmochim. Acta*, *73*(8), 2332–2346, doi:10.1016/j.gca.2009.02.009.
White, H. K., et al. (2012), Impact of the Deepwater Horizon oil spill on a deep-water coral community in the Gulf of Mexico, *Proc. Natl. Acad. Sci. U.S.A.*, *109*(50), 20,303–20,308, doi:10.1073/pnas.1118029109.
Xiao, Y. K., P. V. Shirodkar, C. G. Zhang, H. Z. Wei, W. G. Liu, and W. J. Zhou (2006), Isotopic fractionation of boron in growing corals and its palaeoenvironmental implication, *Curr. Sci.*, *90*, 414–420.
Yu, J., W. S. Broecker, H. Elderfield, Z. Jin, J. McManus, and F. Zhang (2010), Loss of carbon from the deep sea since the last glacial maximum, *Science*, *330*(6007), 1084–1087.
Zhang, J., P. D. Quay, and D. O. Wilbur (1995), Carbon isotope fractionation during gas-water exchange and dissolution of CO_2, *Geochim. Cosmochim. Acta*, *59*, 107–114.